

Structural and electrical properties of sol-gel prepared semiconducting $\text{YBa}_2\text{Cu}_3\text{O}_{7-x}$ thin films with varying coating numbers for uncooled infrared sensors

Tae-Ho Lee, Sung-Gap Lee* and Hye-Rin Jung

Dept. of Ceramic Engineering, Eng. Res. Inst., Gyeongsang National University, Jinju-Si, Korea

Uncooled pyroelectric infrared based on semiconducting $\text{YBa}_2\text{Cu}_3\text{O}_{7-x}$ (YBCO) thin films have been investigated. YBCO precursor solutions were prepared by sol-gel method and YBCO films were fabricated by the spin coating method and structural and electrical properties with variation of coating number were studied. The crystal structure of the YBCO film annealed at 750 °C was polycrystalline tetragonal phase. The YBCO film coated with 5 times showed the average grain size of 75 nm and thickness of 185nm. Temperature resistance coefficient (TCR), responsivity and detectivity of the YBCO film sintered at 700 °C were $-3\%/^{\circ}\text{C}$, 43.42V/W and $5.34 \times 10^6 \text{ cmHz}^{1/2}/\text{W}$, respectively.

Key words: Semiconducting YBCO, Thin films, Sol-gel, Infrared sensor.

Introduction

Infrared (IR) imaging has the potential to play an equally important role in commercial applications in medical, military and transportation systems. Especially, automobiles equipped with IR imaging capabilities have been envisioned for the near future. This technology has the potential to tremendously improve personal safety by enabling good vision at night and under adverse weather conditions. Infrared images in automobiles may also be an enabling technology for “intelligent super-highways”. However, IR imaging systems currently used by the military or medical are too expensive and requiring the cooling system for consumer applications [1, 2]. Recently, the uncooled and inexpensive IR imaging detectors were studied for applications to various sensor devices [3].

Bolometer IR detectors are detected the change of electrical resistance of thermally isolated material due to temperature change by the incident IR signal. And, bolometer IR detectors have been studied mainly the resistive type which detected the change in resistance of metal, semiconductor and superconductor materials. Also, bolometer IR detectors are characterized by simple manufacturing processes and capable of operating at room temperature [4-6].

Recently, the bolometer IR detectors by using titanium, vanadium oxide and $\text{YBa}_2\text{Cu}_3\text{O}_{7-x}$ (YBCO) thin films have been studied for potential applications. However, titanium thin films, which have the temperature coefficient of resistance of $0.28\%/^{\circ}\text{C}$, show a low sensitivity performance for the incident IR. Vanadium

oxide thin films with a single composition are difficult to produce by the sputtering or implantation method because of compositional instability [7-17]. YBCO, known as a high temperature superconductor. The optical and electronic properties of $\text{YBa}_2\text{Cu}_3\text{O}_{7-x}$ are determined by its oxygen stoichiometry. For $x \approx 0$, YBaCuO possesses an orthorhombic crystal structure, exhibits metallic conductivity, and becomes superconductive upon cooling below its critical temperature. As x is increased to 0.5, the crystal undergoes a phase transition to a tetragonal structure and it exhibits semiconducting conductivity characteristics as it exists in a Fermi glass state. As x is increased further over 0.3 YBaCuO becomes a Hubbard insulator with a well defined energy gap on the order of 1.5 eV. This work utilizes the semiconducting phase of the material [18]. Semiconducting thin film, YBCO possesses a high pyroelectric coefficient at room temperature, two hundred times greater than other thin film materials. Different materials used as bolometers include vanadium oxide VO_x [19-20], amorphous Si [21-22], doped poly Si [23-24], and poly Si-Ge alloys [25-26] have been reported. YBCO films have the temperature coefficient of resistance of $3.5 \sim 4\%/^{\circ}\text{C}$ and low leakage current densities. So YBCO films are available materials for the application of the bolometer IR detectors [27-28].

In this study, semiconducting YBCO thin films were prepared using the sol-gel method, which were spin-coated in the Pt/Ti/SiO₂/Si substrate using YBCO alkoxide solutions. We also investigated the structural and electrical properties of YBCO thin films with variation of annealing temperature for application in IR detectors.

Experimental

Using the sol-gel method, YBCO precursor solutions were prepared from the starting materials yttrium

*Corresponding author:
Tel : +82-10-2686-4427
Fax: +82-55-772-1689
E-mail: lsgap@gnu.ac.kr

acetate tetrahydrate $[Y(CH_3COO)_3 \cdot 4H_2O]$, copper acetate monohydrate $[Cu(CH_3COO)_2 \cdot H_2O]$, and barium hydroxide $[Ba(OH)_2 \cdot 8H_2O]$, in addition to the solvent propionic acid and propylamine. The stoichiometric molar ratio of yttrium acetate, barium hydroxide and copper acetate is 1 : 2 : 3. The oxide concentration of the solution is 0.3 mol/L, with a 6 : 1 ratio of propionic acid to propylamine. Diethanolamine is also used to increase wetting and reduce the surface tension of the solution above the polished substrate. The YBCO precursor solution was passed through a syringe filter and spin-coated on the Pt(200 nm)/Ti(10 nm)/SiO₂(300 nm)/p-Si<100> substrates using a spinner operated at 3,000 rpm for 20 sec to form the first layer. These YBCO films were dried at 200 ~ 250 °C for several minutes in air. This coating/drying procedure was repeated several times (1 ~ 7) to obtain the desired thickness (20 ~ 202 nm). The multicoated thin films were dried at 500 °C for 2 h to remove organic materials, and annealed at 750 °C for 2 h in an Ar/O₂ (30 : 70) atmosphere to crystallize them into a tetragonal structure. The crystalline structures of the YBCO thin films were analyzed using a D8 Discover & General Area Detector X-ray Diffraction System (GADDS-SN002623, XRD) with CuK α emission. The surface and cross-sectional microstructures of the films were examined using field-emission scanning electron microscopy (FE-SEM). The electrodes were fabricated by screen-printing the Ag paste. The electrical properties of the specimens were measured using an LCR meter (Fluke 6306, USA) and an electrometer (Keithley 6517A, USA) for IR detector applications.

Results and Discussion

Measurements from the differential thermal analysis (DTA) and thermogravimetry analysis (TGA) curves of the YBCO solution were collected, and the results are shown in Fig. 1. An endothermic peak due to the evaporation of adsorbed water and solvent was observed at around 150 °C. Due to the decomposition of organic residues, exothermic peaks were observed in the temperature range of 400 °C. The weight loss at around 720 °C was attributed to the decomposition of barium carbonate, which formed during heating [29]. In addition, the small exothermic peak at around 800 °C can be attributed to the formation of a single Y₂O₃ phase [30]. Due to the formation of the polycrystalline YBCO phase, exothermic peaks were observed at around 700 °C because not much weight loss was observed in the TGA curve.

Fig. 2 shows the X-ray diffraction patterns of YBCO thin films coated on a SiO₂/Si substrate with varying coating numbers. YBCO thin films coated once and three times displayed a second and unreacted phase such as BaO₂ due to the insufficient number of coatings. The thin films coated five times showed the

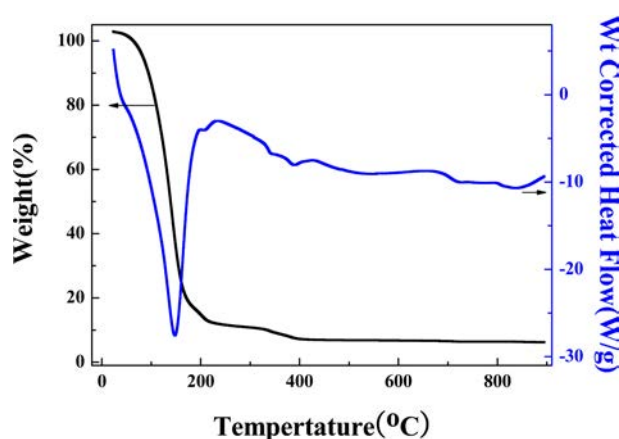


Fig. 1. DTA/TG curves of sol-gel derived YBa₂Cu₃O_{7-x} solution.

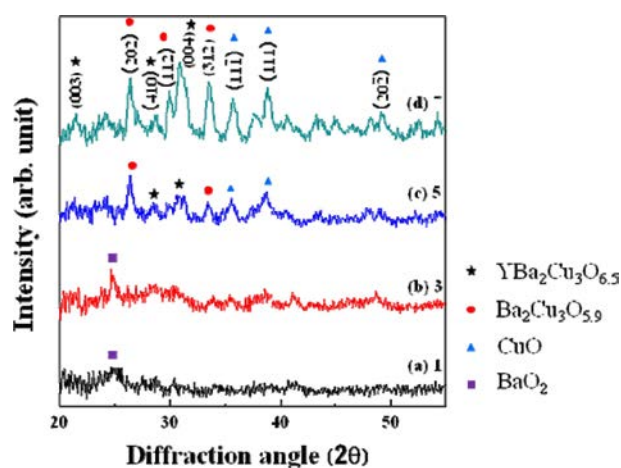


Fig. 2. XRD patterns of YBa₂Cu₃O_{7-x} thin films with variation coating number; (a) 1, (b) 3, (c) 5, (d) 7.

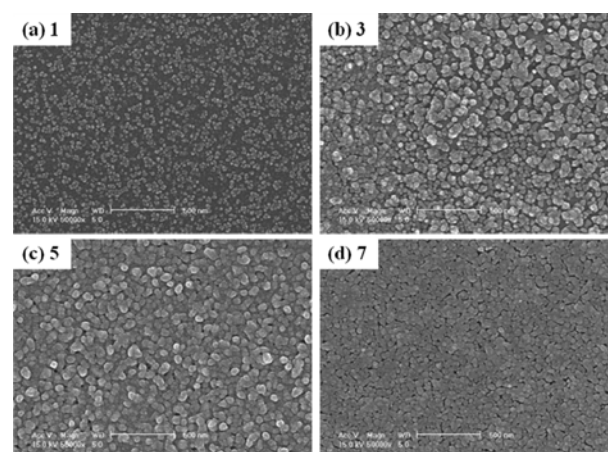


Fig. 3. Surface FE-SEM micrographs of YBa₂Cu₃O_{7-x} thin films with variation coating number; (a) 1, (b) 3, (c) 5, (d) 7.

typical XRD pattern of the tetragonal polycrystalline structure YBa₂Cu₃O_{6.5} and a second phase was also observed. However, the thin film coated seven times showed a second phase such as Ba₂Cu₃O_{5.9} or CuO.

Fig. 3 shows surface SEM micrographs of YBCO films with varying coating numbers. Grain size

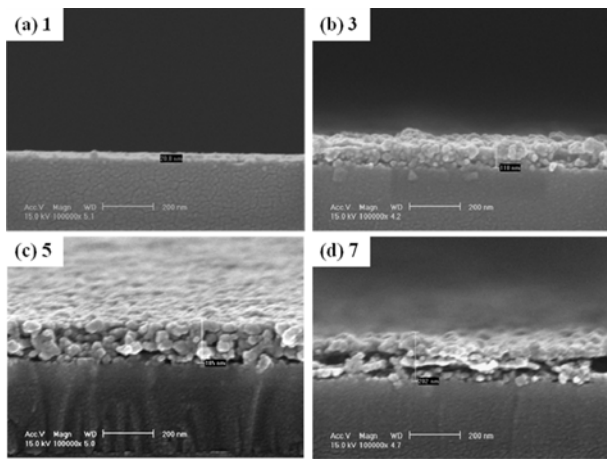


Fig. 4. Cross-sectional FE-SEM micrographs of $\text{YBa}_2\text{Cu}_3\text{O}_{7-x}$ thin films with variation coating number; (a) 1, (b) 3, (c) 5, (d) 7.

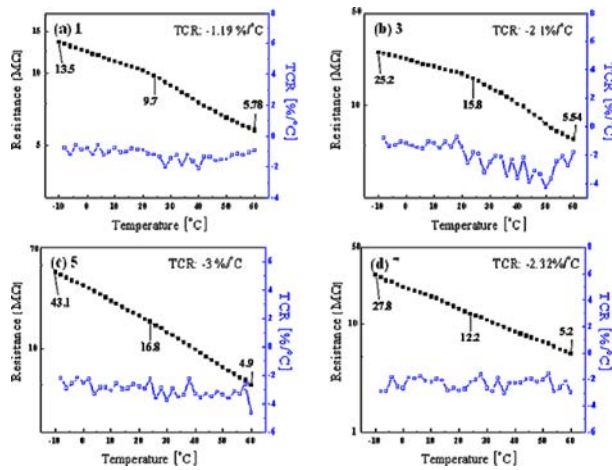


Fig. 5. Resistance and TCR of $\text{YBa}_2\text{Cu}_3\text{O}_{7-x}$ thin films with variation coating number; (a) 1, (b) 3, (c) 5, (d) 7.

increased with an increase in coating number, and the YBCO thin films coated five times showed an average grain size of 75 nm and a smooth surface. The YBCO thin films coated once and three times showed a small grain size due to an insufficient number of coatings. Furthermore, the film coated seven times showed a smaller grain size than that of the film coated 5 times due to a layer of the thin film collapsing.

Fig. 4 shows cross-sectional SEM micrographs of YBCO thin films with varying coating numbers. The thickness of all the films (1 ~ 7 coatings) were 20.8, 110, 185, and 202 nm. Thickness increased with an increase in coating number, and the YBCO thin films coated seven times showed a thickness of 202nm. However, the YBCO thin films coated seven times showed a layer of thin film that had collapsed.

Fig. 5 shows the temperature coefficient of resistance (TCR) of YBCO thin films with varying coating numbers. All YBCO films displayed NTCR (negative temperature coefficient of resistance) properties, which means that electrical resistance decreased with an increase in temperature, typical of semiconductor

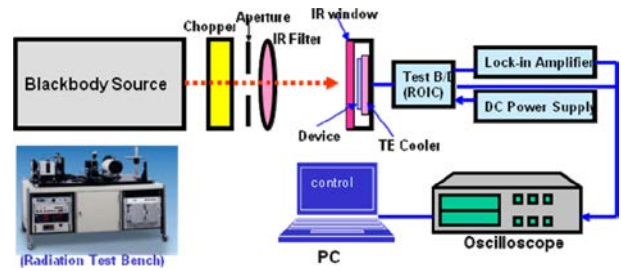


Fig. 6. Measurement set-up for IR device characterization.

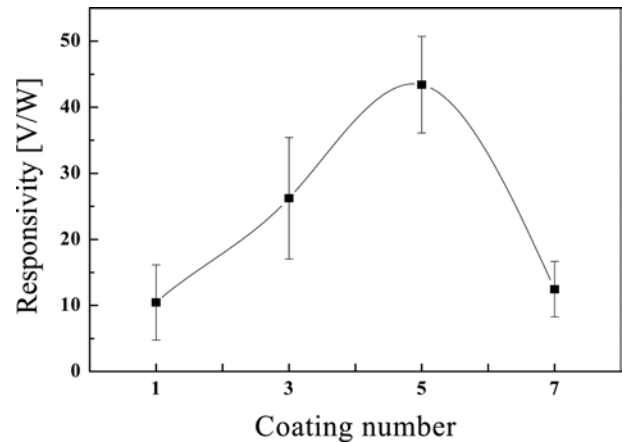


Fig. 7. Responsivity of $\text{YBa}_2\text{Cu}_3\text{O}_{7-x}$ thin films with variation coating number.

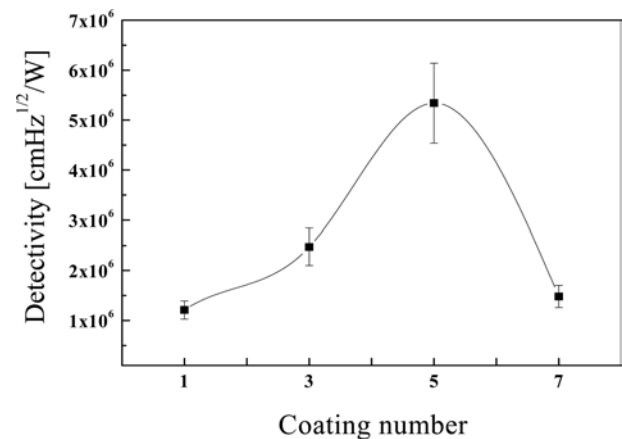


Fig. 8. Detectivity of $\text{YBa}_2\text{Cu}_3\text{O}_{7-x}$ thin films with variation coating number.

materials. Electrical resistance and TCR increased with an increase in the coating number, and the YBCO films coated five times showed the highest values of 16.8MΩ and $-3\%/^{\circ}\text{C}$ at room temperature, respectively. This is due to the small grain size and smooth surface with an increase in coating number, as shown in Fig. 3. However, in the films coated seven times, electrical resistance and TCR decreased due to the layer of thin film collapsing.

A sensing element performance evaluation system, as shown in Fig 6, was used to evaluate the responsivity and detectivity performance of the YBCO thin film IR

Table 1. Measuring parameters.

BBS Temperature	500 °C
Chopper Frequency	15 Hz
BBS Aperture	0.6
Bias Voltage	1 V
Gain	25
Filter	9.46 μm/9.00 ~ 10.0 μm
Distance	3 cm

devices, and a blackbody source furnace at a temperature of 500 °C was used to measure the pyroelectric characteristics of YBCO thin films in the system. The measurement set-up is shown in Fig. 6. Fig. 7 and Fig. 8 show the voltage responsivity and detectivity of YBCO thin films with varying coating numbers. Voltage responsivity, R_v , which is the ratio of the output voltage by the pyroelectric effect to the incident radiant power, was calculated using Eq. (1).

$$R = \frac{V_s}{EA_D} [V/W] \quad (1)$$

where V_s is the signal output, V_N is the noise output, A_D is the detector area, E is the irradiance, and Df is the effective radiation bandwidth. Detectivity, D^* , which is the signal-to-noise ratio of the detector when an incident infrared beam is radiated per unit area, was calculated using Eq. (2).

$$NEP = EA_D \left(\frac{V_N}{V_s} \right) \quad D^* = \frac{\sqrt{\Delta f A_D}}{NEP} [\text{cm Hz}^{1/2} \text{W}^{-1}] \quad (2)$$

Table 1. shows the measuring parameters for responsivity and detectivity.

The YBCO thin films coated five times showed maximum values of 43.42 V/W and $5.34 \times 10^6 \text{ cmHz}^{1/2}/\text{W}$, respectively. The maximum voltage responsivity and detectivity were due to the high TCR and electrical resistance, as shown in Eq. (1). Furthermore, the semiconducting YBCO single phase displayed excellent electrical properties, as shown in Fig. 5.

Conclusions

In this study, we fabricated semiconducting YBCO thin films using the spin-coating method. The YBCO thin films were coated once to seven times. Crystallization of the YBCO thin films was severely affected by the coating number and the films coated five times displayed a tetragonal polycrystalline structure. Pores in the IR detector materials prevent the dispersion of the incident IR, decreasing the sensitivity of the IR detectors. The temperature resistance coefficient, responsivity and detectivity of the YBCO film coated five times were $-3\%/^{\circ}\text{C}$ at room temperature, 43.42 V/W and $5.34 \times 10^6 \text{ cmHz}^{1/2}/\text{W}$, respectively.

Acknowledgments

This work was supported by the Korea Research Foundation (KRF) grant funded by the Korea government (MEST) (No. 03-2011-0223).

References

1. F. Niklaus, C. Vieider and H. Jacobsen, Proc. SPIE 6836 (2007) 0D1..
2. L. Luo, M. E. Hawley, C. J. Maggiore, R. C. Dye and R. E. Muenchausen, Appl. Phys. Lett. 62 (1993) 485.
3. P.-Y. Chu and R. C. Buchaman, J. Mater. Res. 8 (1993) 2134.
4. P. C. McIntyre, M. J. Cima, J. A. Smith, R. B. Hallock, M. P. Siegal and J. M. Phillips, J. appl. Phys. 71 (1992) 1868.
5. A. Jahanzeb, C. M. Travers, D. P. Butler, Z. Celik-Butler and J. E. Gray, Appl. Phys. Lett. 70 (1997) 3495.
6. A. Aligia and J. Garces, Phys. Rev. B 49 (1994) 524.
7. N. A. Khan, M. Z. Iqbal and N. Baber, Solid State Commun. 92 (1994) 607.
8. John E. Gray, Zeynep Celik-butler and Donald P. Butler, IEEE J. Microelectromech. Syst., 8 (1999) 192-199.
9. S. Verghese, P. L. Richards, K. Char, and S. A. Sachtjen, IEEE Trans. Magn., 27 (1991) 3077.
10. B. R. Johnson, T. Ohnstein, C. J. Han, R. Higashi, P. W. Kruse, R. A. Wood, H. Marsh, and S. B. Dunham, IEEE Trans. Appl. Superconduct., 3 (1993) 2856-2859.
11. T. G. Stratton, B. E. Cole, P. W. Kruse, R. A. Wood, K. Beauchamp, T. F. Wang, B. Johnson, and A. M. Goldman, Appl. Phys. Lett., 57 (1990) 99-100.
12. Q. Li, D. B. Fenner, W. D. Hamblen, and D. G. Hamblen, Appl. Phys. Lett., 62 (1993) 2428-2430.
13. M. C. Foote, B. R. Johnson, and B. D. Hunt, Proc. SPIE, 2159 (1994) 2-9.
14. J. P. Rice, E. N. Grossman, and D. A. Rudman, Appl. Phys. Lett., 65 (1994) 773-775.
15. C. A. Bang, J. P. Rice, M. I. Flik, D. A. Rudman, and M. A. Schmidt, IEEE J. Microelectromech. Syst., 2 (1993) 160-164.
16. M. Nahum, Q. Hu, P. L. Richards, S. A. Sachtjen, N. Newman, and B. F. Cole, IEEE Trans. Magn., 27 (1991) 3081-3084.
17. R. Barth, J. Siewert, C. Jaekel, B. Spangenberg, H. Kurz, W. Prusseit, B. Utz, and H. Wolf, J. Appl. Phys., 78 (1995) 4218-4221.
18. A. Dasgupta, S. Ghosh, and S. Ray, J. Mater. Sci. Lett. 14 (1995) 1037.
19. S. Mathews, Thermal imaging on the rise, Laser Focus World 40 (2004) 105-107.
20. W. Radford, D. Murphy, M. Ray, S. Propst, A. Kennedy, J. Kojiro, J. Woolayaw, K. Soch, R. Coda, G. Lung, E. Moody, D. Gleichman, S. Baur, SPIE Proc. 2746 (1996) 82-92.
21. J. Brady, T. Schimert, D. Ratcliff, R. Gooch, B. Ritchey, P. McCardel, K. Rachels, S. Ropson, M. Wand, M. Weinstein, J. Wynn, SPIE Proc. 3689 (1999) 161-167.
22. T. Schimert, D. Ratcliff, J. Brady, S. Ropson, R. Gooch, B. Ritchey, P. McCardel, K. Rachels, M. Wand, M. Weinstein, J. Wynn, SPIE Proc. 3713 (1999) 101-111.
23. M.S. Liu, J.S. Haviland, C.J. Yue, Intergrated Infrared Sensitive Bolometers, Patent No. US005260225A (1992).
24. P. Fiorini, S. Sedky, M. Caymax, C. Baert, Patent No. US009194722B1 (2001).

25. J. Wauters, *Laser Focus World* 33 (1997) 145-148.
26. A. Tanaka, S. Matsumoto, N. Tsukamoto, S. Itoh, T. Endoh, A. Nakazato, Y. Kumazawa, M. Hijikawa, H. Gotoh, T. Tanaka, N. Teranishi, *Tech. Digest*, in: *International Conference on Solid-State Sensors and Actuators and Eurosensors IX*, vol. 2, Stockholm, Sweden, June 25-29 (1995) 632-635.
27. M. Longhin, A. J. Kreisler, and A. F. Degardin, *Materials Science Forum* 587 (2008) 273.
28. A. Mahmood, D. P. Butler, and Z. Celik-Butler, *Sens. Actuators A*, 132 (2006) 452.
29. T. Hayashi, H. Shinozaki, K. Sasaki, *Jap. J. Appl. Phys.* 37 5232 (1998).
30. T. T. Thuy, S. Hoste, G. G. Herman, K. De Buysser, P. Lommens, J. Feys, D. Vandeput, I. Van Driessche, *J Sol-Gel Sci Technol*, 52 (2009) 124.